Process Mining Analytics for Industry 4.0 with Graph Signal Processing

Georgios Drakopoulos[1][a], Eleanna Kafeza[2][b], Phivos Mylonas[1][c] and Spyros Sioutas[3]

[1]*Department of Informatics, Ionian University, Greece*

[2]*College of Technology and Innovation, Zayed University, U.A.E.*

[3]*Computer Engineering and Informatics Department, University of Patras, Greece*

Keywords: Process Mining, Industry 4.0, Graph Signal Processing, Graph Mining, Multilayer Graphs, PM4Py, Neo4j.

Abstract: Process mining is the art and science of (semi)automatically generating business processes from a large number of logs coming from potentially heterogeneous systems. With the recent advent of Industry 4.0 analog enterprise environments such as floor shops and long supply chains are bound to full digitization. In this context interest in process mining has been invigorated. Multilayer graphs constitute a broad class of combinatorial objects for representing, among others, business processes in a natural and intuitive way. Specifically the concepts of state and transition, central to the majority of existing approaches, are inherent in these graphs and coupled with both semantics and graph signal processing. In this work a model for representing business processes with multilayer graphs along with related analytics based on information theory are proposed. As a proof of concept, the latter have been applied to large synthetic datasets of increasing complexity and with real world properties, as determined by the recent process mining scientific literature, with encouraging results.

1 INTRODUCTION

Recently the theory and practice of manufacturing underwent a series of radical evolutionary transformations after a long period covering Antiquity and the Middle Ages where humans, whether slaves or highly paid technicians and professionals, animals, and simple machines such as Heron's steam engine or *Aeolipile* were the primary means of production. The roots of each major milestone can be respectively traced in the following historical periods:

- The Victorian era[1] in the wake of a major scientific wave saw the massive transition to hydraulic power for a broad spectrum of applictions. The uncontested colophon of that era was the development of steam engine.

- Between the French-Prussian war of 1871 up to the start of First World War in 1914 heavy emphasis was placed on developing extensive networks, whether physical, such as railroads and post offices, or telecommunication ones, like the telegraph and local telephone systems. These networks prompted the construction of massive assembly lines and supply chains.

- Finally, after the end of the Second World War in 1945 and until the beginning of the 21st century focus shifted on digitization and miniaturization, eventually giving rise to microelectronics and digital computers. The main paradigm shift here was the reinforcement not only of the human body but of the brain as well.

Currently Industry 4.0, originally a set of specifications compiled in 2011 by the *Bundesregierung*, namely the federal German government, aims to transform manufacturing landscape by introducing the use of sensors, artificial intelligence (AI), and Internet of Things (IoT) technology in order to increase productivity, cybersecurity, and personnel safety. In this way diverse operational objectives from various scopes can be achieved even under quite adverse circumstances. At the same time human-to-machine and machine-to-machine will become seamless and more efficient through wearable electronics for humans and reconfigurable sensor arrays for machines.

In this digital enterprise setting the role of process mining is becoming increasingly more important as large event logs are created by a multitude of commer-

[a] https://orcid.org/0000-0002-0975-1877

[b] https://orcid.org/0000-0001-9565-2375

[c] https://orcid.org/0000-0002-6916-3129

[1]The technology of that era and the promises it brought about human life led to the *steampunk* subculture and literary genre.

cial business applications and big process graphs are generated for various production purposes. Given that data volume and its high generation rate, errors are almost bound to happen. They are frequently manifested in the absence or addition of spurious vertices or edges at the process graphs. However, a more insidious result is the changes to process graph semantics as errors are more subtle and can be thus propagated undetected in the process graph.

The primary research objective of this conference paper is the development of edge, path, and triangle similarity metrics for evaluating the difference between any template process graph and a corresponding variant one. Said difference is evaluated with a metric enriched with semantics represented as edge labels which is derived from information theory. This work differentiates from previous approaches in two ways, namely the use of multilayer graphs in order to represent long Industry 4.0 processes and the use of the emerging field of graph signal processing (GSP).

The remaning of this work is structured as follows. In Section 2 the recent scientific literature pertaining to process mining and multilayher graphs is briefly reviewed. Section 3 contains the formal definition of as well as some intuituion about mulilayer graphs. The proposed methodology is described in detail in section 4. The results of applying it to synthetic process benchmark graphs of increasing complexity are given in section 5. Section 6 recapitulates the main results and outlines future research directions. Technical acronyms are defined the first time they are encountered in the text. In definitions parameters are given after formal arguments following a semicolon. Finally, table 1 summarizes the notation of this work.

Table 1: Notation of this conference paper.

Symbol	Meaning	First
$\overset{\triangle}{=}$	Equality by definition	Eq.(1)
$\{s_1,\ldots,s_n\}$	Set with $s_1,\ldots,s_n$	Eq.(2)
$(t_1,\ldots,t_n)$	Tuple with $t_1,\ldots,t_n$	Eq.(1)
$|S|$	Set or tuple cardinality	Eq.(3)
$\text{logit}(p)$	Logit function	Eq.(5)
$[e_1,\ldots,e_p]$	Path of edges $e_1,\ldots,e_p$	Eq.(12)
$\mathcal{H}(\cdot)$	Harmonic mean	Eq.(5)

2 PREVIOUS WORK

Industry 4.0 is a major milestone in the history of industrial organization and production (da Rosa Righi et al., 2020). It aims to the full digitization of industrial production through a wide array of sensors installed in machinery and in wearable electronics

for human operators as well as through delegation of minor, mundane, or dangerous tasks to computer-operated equipment (Bigliardi et al., 2020). Various sensor architectures based on the Industry 4.0 requirements have been proposed and compared in (Bajic et al., 2020). Operational criteria and considerations for the industrial equipment are examined in (Culot et al., 2020). The connections between Industry 4.0 and circular economy are explored in (Rajput and Singh, 2019). The principal question of sustainability is put in (Bai et al., 2020). An extensive review of the relevant bibliography about Industry 4.0 is given in (Souza et al., 2020).

Process mining relies heavily on the parsing of automatically generated process logs in order to discover patterns, latent dependencies, and persistent anomalies (Mitsyuk et al., 2017; Reinkemeyer, 2020). The IEEE extensive event stream (XES) or IEEE standard 1849-2016 is a standard log file format designed for the explicit purpose of process mining proposed in (Acampora et al., 2017). Automated log mining is explained in (Egger et al., 2020). PM4py is a Python package for process mining complete with methods for pattern discovery and miners such as A and A$^+$ (Berti et al., 2019). Dealing with malformed or otherwise imperfect process logs is examined in (Suriadi et al., 2017). Context-aware process mining with the introduction of advanced graph mining is the topic of (Becker and Intoyoad, 2017). The role of process mining to auditing information systems is described in (Zerbino et al., 2018). Finally, among the various surveys covering the topic are (Lopes and Ferreira, 2019) and (Verenich et al., 2019).

Multilayer or multiplex graphs allow parallel edges between the same pairs of vertices (Caimo and Gollini, 2020; Halnaut et al., 2020). As with ordinary graphs massive graph mining for this class can take place with the help of graph analytics (Zhou and Cheung, 2019) including attribute engineering (Drakopoulos and Mylonas, 2020). Also multilayer graphs have been proposed as a scalable IoT model (Xie et al., 2020). Functional and structural aspects of brain circuits are combined to form multilayer graphs in (Mandke et al., 2018). Visualization techniques for multilayer graphs are explored in (McGee et al., 2019). Semi-supervised learning methods for this class of graphs are proposed in (Mercado et al., 2019). Multilayer graphs have been used for image segmentation (Wang et al., 2016), spectral graph clustering (Chen and Hero, 2017), fast graph transform mining (Drakopoulos et al., 2021). A versatile, presistent, and space efficient data structure for process storage is proposed in (Kontopoulos and Drakopoulos, 2014).

3 MULTILAYER GRAPHS

Informally speaking, the class of multilayer graphs represents graphs with multiple edge labels. The name comes from the fact when considering only a single given label, then an ordinary graph termed a *layer* results. Thus, a multilayer graph can be decomposed to various layers. The total activity in such a graph comes from the following interacting factors:

- Activity in each separate layer. This happens at the vertices and edges of the specific layer.

- Activity across layers. Typically this takes place at the vertices belonging to at least two layers.

The above imply that any extension of Metcalfe's law (Metcalfe, 2013) to multilayer graphs should take into account both these factors if the true graph value is to be determined. Possibly this entails a composite power law which will be a function of the overall average degree or the average degree of each layer.

Formally, the combinatorial structure of a multilayer graph is given by definition 1.

Definition 1 (Mutilayer graph). *A multilayer graph is the ordered quadruple of equation* (1).

$$G \stackrel{\triangle}{=} (V, E, L, h) \qquad (1)$$

In equation (1) *the tuple elements are the following:*

- *The vertex set V contains the vertices of the graph. In this context vertices represent special states, namely the beginning or the end of a process or important intermediate steps.*

- *The edge set $E \subseteq V \times V \times L$ contains the labeled edges of the graph. They indicate dependencies or the various connections between either process states or entire processes.*

4 PROPOSED METHODOLOGY

4.1 General Notes

In this section the proposed methodology based on the class of multilayer graphs will be described. First the way edge similarity is computed will be presented followed by applications to paths and triangles, two of the most common structural patterns encountered in process mining graphs. Then the edge signal to noise ratio, a concept borrowed and adapted from the field of information theory, will be also presented.

At this point it is important to highlight that the theory developed here is based on the following underlying fundamental assumption.

Assumption 1 (Alignment assumption). *The template and the variant process graphs are aligned.*

This is not a trivial observation as alignment is a major research topic in graph mining, ontology discovery, and in related fields (Dasiopoulou et al., 2008). The approaches range from combinatorial to linear algebraic and signal processing ones.

Moreover, emphasis should be placed that the comparison metrics described in this section were explicitly designed for evaluating distances between the original process graph and the variant graph, explained respectively in definitions 2 and 3.

Definition 2 (Process graph). *The process graph is the template describing in detail the desired process mining assumptions, approach, and operational characteristics of an organization.*

Definition 3 (Variant graph). *The variant graph is the process mining graph constructed (semi)automatically from parsing process logs, equipment sensors, personnel reports, and any other technical means deployed in the field.*

Since the original process graph and any variant one deriving from it are aligned, each edge e in the latter has a unique counterpart e_0 in the former. Hence it makes perfect sense to refer in the text to the counterpart of e without any further clarification.

4.2 Edge SNR

Since multilayer graphs allow multiple edges between the same pair of vertices, for comparison purposes as well as for notation simplification a group of labeled edges can be replaced with a single edge with a set, the *edge set*, containing the labels of the respective individual edges. In figure 1 is shown how various parallel labeled edges can be substituted with an equivalent label set. This step is crucial for developing the analytics presented in later sections.

Therefore, in a process graph for a given vertex pair a group of connecting edges $e_1, \ldots, e_n$ with corresponding labels $l_1, \ldots, l_n$ L is replaced by a single edge e with the edge set of equation (2):

$$L \stackrel{\triangle}{=} \{l_1, \ldots, l_n\} \qquad (2)$$

The basic building block for assessing the similarity between process patterns is edge similarity. In order to evaluate the similarity between two edges, one from the process graph and one from the template graph, it suffices to compare the respective label sets. To this end the asymmetric Tversky index will be employed. The latter evaluates the divergence between two sets T and V where the former is considered to be a template and the latter a variance thereof. Thus
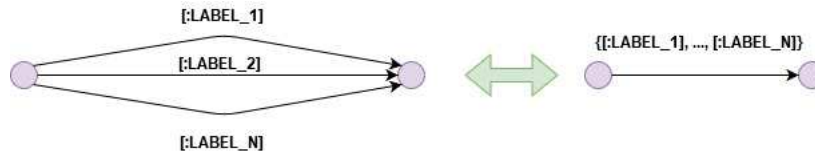
Figure 1: Construction of the edge label set. Source: Authors.

these two sets are by construction not interchangeable. This fundamental property is reflected in the index mathematical definition (Tversky, 1977):

$$\tau(T, V; \alpha_0, \beta_0) \triangleq \frac{|T \cap V|}{|T \cup V| + \alpha_0 |T \setminus V| + \beta_0 |V \setminus T|}$$
(3)

In equation (3) the parameters α_0 and β_0 denote respectively the weights for the number of elements present in T but absent in V and vice versa. Although their only real constraint is that they are non-negative, frequently their sum is normalized to one such that α_0 and β_0 become relative weights. This is further illustratred by typically selecting their values such that their ratio takes a predetermined and application-dependent value γ_0 as shown in equation (4):

$$\frac{\alpha_0}{\beta_0} = \gamma_0$$
(4)

These changes to process graphs labels can be thought of as noise similar to that present in digital electronics-based wired (DEBW) telecommunications systems. Although based on this observation certain concepts such the signal-to-noise ratio (SNR) can be defined, the label noise is fundamenally different because of the following reasons:

- In contrast to DEBW systems where the primary source of noise is continuous due to the nature, the complexity, and the cumulative effect of electronic components, any changes to edge labels under the proposed model are discrete.

- In DEBW systems the noise is arithmetic in nature and leads to probabilistic errors, where in process graphs the label noise under consideration is categorical and results in semantic errors. Still the latter can be probabilistically represented.

- In DEBW systems noise comes from the electronics components located in the transmitter and the receiver or from the propagation medium, whereas changes to labels stem primarily from design or communication errors.

Given the above it is clear that the additive white Gaussian noise (AWGN) model is not appropriate in this context and by extension neither is the Gaussian distribution a proper model for the label noise.

SNR is a fundamental concept in information theory which serves in the development for metrics of signal distorion over telecommunication channels.

Definition 4 (Edge SNR). *For a single edge of the variant process graph the SNR is defined as the logarithm of the ratio of to as shown in equation* (5). *The edge SNR is always relative to an aligned reference template graph and e_0 is the corresponding edge to e.*

$$s(e; e_0) \triangleq \ln\left(\frac{\tau(L, L_0)}{1 - \tau(L, L_0)}\right) = \operatorname{logit}(\tau(L, L_0)) \quad (5)$$

The intuition behind equation (5) is that $s(e)$ is the order of magnitude of the similarity between the process edge and its template divided by their respective distance. Both the similarity and the distance are quantified with the Tversky index, which leads to the special form of the SNR. By construction said index lies between zero and one, which also gives rise to the question whether this imposes lower and upper limits to SNR, both desirable in many engineering settings.

The SNR of definition 4 is an odd function around the axis $x_0 = 1/2$, namely the middle point of the range of the Tversky index, as shown in equation (6):

$$\operatorname{logit}(1 - \tau) = \ln\left(\frac{1 - \tau}{1 - (1 - \tau)}\right) = -\operatorname{logit}(\tau)$$

$$\operatorname{logit}\left(\frac{1}{2}\right) = \ln\left(\frac{\frac{1}{2}}{1 - \frac{1}{2}}\right) = \ln 1 = 0 \quad (6)$$

Among the significant properties of the $\operatorname{logit}(\cdot)$ function, which can serve as building blocks for sophisticated SNR metrics, are the following:

- In general linear regression is the canonical link function of the Bernoulli distribution, meaning that it allows linear regression when the output is a binary or Bernoulli random variable.

- It is the inverse of the standard logistic function $\varphi(\cdot)$ shown in equation (7). Therefore, $\operatorname{logit}(\cdot)$ maps logistically distributed input to the real axis.

$$\varphi(x; \lambda_0) \triangleq \frac{1}{1 + \exp(-\lambda_0 x)} \quad (7)$$

- It roughly approximates the information content of the ratio of two random samples, one from a logistic distribution and one from its reflection.

- Moreover, the $\operatorname{logit}(\cdot)$ can be approximated by a rescaled $\operatorname{probit}(\cdot)$ function. This can be useful when the Tversky index in definition 4 is close to its domain limits to ensure numerical stability.

In equation (5) the selection of the logarithm base does not have any effect on the outcome besides rescaling it, which is tantamount to selecting the units in which the SNR is expressed as shown in equation (8). The natural logarithm in definition 4 has been selected because of its algorithmic properties.

$$\log_a b = \frac{\log_c a}{\log_c b}, \qquad a, b, c \neq 0 \qquad (8)$$

The numerical behavior of s with respect to $\tau(L, L_0)$ in equation (5) is degrading as label noise vanishes or as it creates excessive divergence from the template edge as shown in equation (9):

$$\frac{\partial s}{\partial \tau} = \frac{1}{\tau(1-\tau)} = \frac{1}{\tau} + \frac{1}{1-\tau} \qquad (9)$$

From equation (9) it can be seen that the first derivative of the edge SNR can be interpreted as the sum of two equivalent hyperbolic modes which are also reflections of each other. Moreover, the form of (9) is a direct consquence of the fact that $\mathrm{probit}(\cdot)$ is the inverse of the standard logistic function $\varphi(x)$ as mentioned earlier. Recall that $\varphi(x)$ is the non-singular solution of the non-linear differential equation of (10), connecting $\varphi(x)$ with Verhulst population models:

$$\varphi^{(1)}(x) = \varphi(x)(1 - \varphi(x)) \qquad (10)$$

The second derivative of the edge SNR can be computed from equation (9) yielding equation (11):

$$\frac{\partial^2 s}{\partial \tau^2} = \frac{2\tau - 1}{\tau^2(1-\tau)^2} = \frac{1}{(1-\tau)^2} - \frac{1}{\tau^2} \qquad (11)$$

Equation (11) is essentially an inverse cubic function with each of the two poles of (9) having a multiplicity of two. Moreover, it changes sign when τ is around the single zero $1/2$. When $1 - \tau$ is treated as a pseudoindepedent variable, then the second edge SNR derivative becomes a hyperbola in the axes of τ (secondary) and its reflection $1 - \tau$ (primary).

In figure 2 the edge SNR of equation (5) and its first derivative of equation (9) are shown. The latter has been rescaled and translated so that both are zero when the Tversky index equals $1/2$

4.3 Path SNR

Given that most non-trivial industrial processes take more than a singe step to complete, it makes perfect sense to extend the SNR of definition (5) to more than one edges. In this subsection the case of linear directed paths, meaning they contain neither crossings nor cycles, of arbitrary length is examined. Initially, let p be a directed path in a process graph consisting of n labeled edges as shown in equation (12):

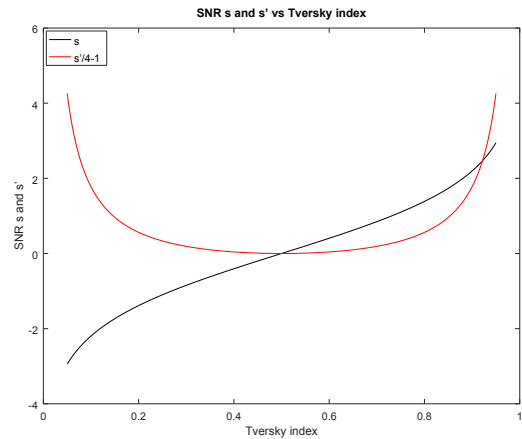$$p \overset{\triangle}{=} [e_1, \ldots, e_n] \qquad (12)$$

Figure 2: Label SNR vs Tversky index. Source: Authors.

The formal description of the SNR for an entire path in the above sense is given in definition 5.

Definition 5 (Path SNR). *The SNR of a linear directed path of a variant process graph relative to an aligned template graph is the harmonic mean of the individual SNRs of the edges constituting that path.*

$$s(p) \overset{\triangle}{=} \frac{n}{\sum_{k=1}^{n} \dfrac{1}{s(e_k)}} \overset{\triangle}{=} \mathcal{H}(s(e_1), \ldots, s(e_n)) \quad (13)$$

The harmonic mean of equation (13) has been selected because of its many appealing algorithmic and numerical properties. Specifically:

- It is robust to any zero or near zero, namely close to machine precision, values of $s(e_k)$. In the limiting case, it handles edges with no similarity with their corresponding ones in the template graph.

- It is symmetric with respect of the individual edge SNRs. Moreover, the order in which the denominator terms has no effect. Therefore, similar paths are expected to have similar SNRs.

- Since the order of the denominator summands is irrelevant, numerical phenomena like catastrophic cancellation can be avoided by employing stable numerical algorithms such as Priest summation.

- The harmonic mean is relatively insensitive to any outliers and therefore it is considered to yield a more representative value out of a given set of numbers while respecting certain distributions.

The vector of independent variables $\mathbf{s}$ contains the SNR of each individual edge of the path p under consideration. The differentiation of $s(p)$ in equation (15) and (16) will be with respect to this vector.

$$\mathbf{s} \overset{\triangle}{=} \begin{bmatrix} s(e_1) & \ldots & s(e_n) \end{bmatrix}^T \qquad (14)$$

The Jacobian vector **h** of (13) consists of the vector of the partial first derivatives as shown in (15). Its interpretation is that it represents the local gradient.

$$
\begin{aligned}
\mathbf{h} &\triangleq \nabla_{\mathbf{s}} s(p) \\
&= \begin{bmatrix} \dfrac{\partial s(p)}{\partial s(e_1)} & \dfrac{\partial s(p)}{\partial s(e_2)} & \cdots & \dfrac{\partial s(p)}{\partial s(e_n)} \end{bmatrix}^T \\
&= \dfrac{n}{\left(\sum_{k=1}^{n} \dfrac{1}{s(e_k)} \right)^2} \begin{bmatrix} \dfrac{1}{s(e_1)^2} \\ \vdots \\ \dfrac{1}{s(e_n)^2} \end{bmatrix}
\end{aligned} \tag{15}
$$

The symmetry of the path SNR is reflected in the Jacobian vector which is isotropic. Therefore the gradient is independent of the way the path SNR is approached but instead depends on the distance from the point the gradient refers to. The Hessian matrix **H** of (13) can be computed from (15) giving (16). The Hessian represents the local curvature of $s(p)$.

$$
\begin{aligned}
\mathbf{H} &\triangleq \nabla_{\mathbf{s}} \nabla_{\mathbf{s}}^T s(p) \\
&= \begin{bmatrix} \dfrac{\partial^2 s(p)}{\partial s(e_1)^2} & \cdots & \dfrac{\partial^2 s(p)}{\partial s(e_1)\partial s(e_n)} \\ \dfrac{\partial^2 s(p)}{\partial s(e_2)\partial s(e_1)} & \cdots & \dfrac{\partial^2 s(p)}{\partial s(e_2)\partial s(s_n)} \\ \vdots & \ddots & \vdots \\ \dfrac{\partial^2 s(p)}{\partial s(e_n)\partial s(e_1)} & \cdots & \dfrac{\partial^2 s(p)}{\partial s(e_n)^2} \end{bmatrix}
\end{aligned} \tag{16}
$$

The Hessian elements are computed as follows:

$$
\mathbf{H}[i,j] = \begin{cases} \dfrac{4n}{s(e_i)^5} \dfrac{1 - \dfrac{s(e_i)^2}{2}\sum_{k=1}^{n}\dfrac{1}{s(e_k)}}{\left(\sum_{k=1}^{n}\dfrac{1}{s(e_k)}\right)^3} & ,i = j \\[4ex] \dfrac{4n}{s(e_i)^2 s(e_j)^3} \dfrac{1}{\left(\sum_{k=1}^{n}\dfrac{1}{s(e_k)}\right)^3} & ,i \neq j \end{cases} \tag{17}
$$

From the form of the Hessian matrix the following observations can be made:

- The path length n plays a role in local curvature. Thus long paths tend to have more curvature.
- Each edge contributes not only to local but also to global patterns.

4.4 Triangle SNR

Triangles are the simplest yet most fundamental community blocks in graphs as well as the first closed graph structural pattern. By extending the path SNR metric to any given triangle T yields equation (18):

$$
s(T) \triangleq \mathcal{H}(s(e_1), s(e_2), s(e_3)) \tag{18}
$$

A major property of graph triangles, especially in the broad class of power law or scale free graphs, is that despite their small size they constitute important structural components. Triangles contribute to the global graph modularity and compactness because they are locally interwoven. This provides multiple alternative short paths between a number of vertices which are frequently resilient to the deletion of a small number of local and non-bridge edges.

5 RESULTS

In this section the similarity metrics presented earlier are put to test. Synthetic datasets based on the following real world Industry 4.0 requirements were constructed. Specifically, the benchmarks will be graph datasets generated to have many of the process graph properties reported in the recent process mining scientific literature in works such as (Verenich et al., 2019) and (Acampora et al., 2017). These include:

- The total number of vertices and edges as well as the number of labels of the template graph.
- The average graph diameter as well as the effective 70%, 80%, and 90% graph diameters.
- The expected number of triangles, which is a major indicator of graph structural coherence.
- The expected path length and the associated variance, which reveals local and global information.

Table 2 contains the synopses of template graphs used in this work. Each is a Kronecker graph coming from a generator graph of lower size. In order to create the variant graphs labels where either added or removed at random from edges of the template graph. Label addition and removal was done with the Poisson distribution of equation (19) with μ_0 equal to the mean number of labels in each graph.

$$
p_k \triangleq \dfrac{\mu_0^k}{k!} e^{-\mu_0} \tag{19}
$$

For each template graph ten thousand instances were created. The average values and the respective variances for each metric were recorded. Coding was done in Python 3.8 with the numpy and the scipy packages for analysis. Graphs were created and handled with the NetworkX package.

Table 2: Dataset properties.

Property	Set 1	Set 2	Set 3	Set 4
Generator vertices	5	5	7	7
Generator edges	7	8	13	17
Template vertices	3125	15625	16807	16807
Template edges	16807	262144	371293	1419857
Label set size	16	32	48	64
Labels per edge	6.53	11.67	28.44	32.33
Diameter	11	13	15	16
80% effective	7	9	11	12
90% effective	8	11	13	15
Number of triangles	625	33125	67617	212881

From the dataset synopses presented in table 2 it follows that they have an increasing level of complexity, implying that more complex datasets pose a bigger challenge for analytics designers.

In figure 3 the average edge SNR as a function of the normalized path legth. Specifically, the path length is expressed as a fraction of the respective graph diameter. It can be seen that edge SNR is a decreasing function of both the overall process graph complexity as well as of the path length. This can be explained as path similarity degrades as more steps as added to an industrial process.
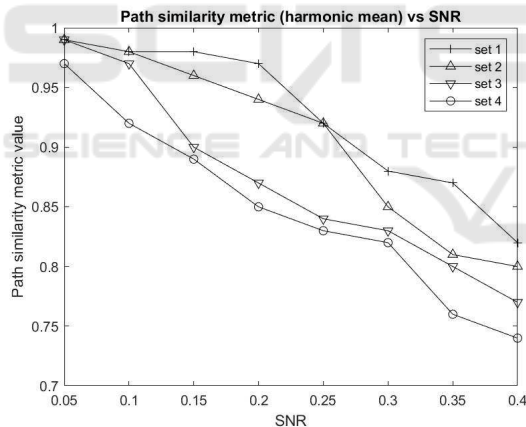

Figure 3: SNR vs path length. Source: Authors.

6 CONCLUSIONS

This conference paper focuses on a process mining model for Industry 4.0 based on the class of multilayer graphs as well as on associated analytics. This class of graphs extends the ordinary ones by adding edge labels, essentially semantics based on the underlying process logs. This is appealing since edges can have properties depending on their role in the overall process and, moreover, edges denoting tasks executed in parallel along the same check points can

be combined to a single one with a label set. As high degree task parallelism, typically due to multiple sensor readings, is a very common characteristic of an Industry 4.0 setting, edges with label sets of even a moderate size arise frequently. In turn, these sets can be the building blocks for a number of analytics for the distance between the process graph, namely the actual graph as mined from the various system and process logs, and the template graph, namely the blueprint process graph as derived by system designers. Analytics based on this distance metric include path and vertex similarity metrics as well as a modified clustering coefficient. Experiments conducted with synthetic datasets indicate that these analytics can discover errors in multilayer graphs while at the same time being algorithmically robust and numerically stable, given the large number of floating points operations required to derive the final result.

ACKNOWLEDGEMENTS

REFERENCES

Acampora, G., Vitiello, A., Di Stefano, B., van der Aalst, W., Günther, C., and Verbeek, E. (2017). IEEE 1849: The XES standard. *IEEE Computational Intelligence Magazine*, 12(2):4–8.

Bai, C., Dallasega, P., Orzes, G., and Sarkis, J. (2020). Industry 4.0 technologies assessment: A sustainability perspective. *International Journal of Production Economics*, 229.

Bajic, B., Rikalovic, A., Suzic, N., and Piuri, V. (2020). Industry 4.0 implementation challenges and opportunities: A managerial perspective. *IEEE Systems Journal*.

Becker, T. and Intoyoad, W. (2017). Context aware process mining in logistics. *Procedia Cirp*, 63:557–562.

Berti, A., van Zelst, S. J., and van der Aalst, W. M. (2019). PM4Py Web Services: Easy development, integration and deployment of process mining features in any application stack. In *BPM (PhD/Demos)*, pages 174–178.

Bigliardi, B., Bottani, E., and Casella, G. (2020). Enabling technologies, application areas and impact of Industry 4.0: A bibliographic analysis. *Procedia Manufacturing*, 42:322–326.

Caimo, A. and Gollini, I. (2020). A multilayer exponential random graph modelling approach for weighted networks. *Computational Statistics & Data Analysis*, 142.

Chen, P.-Y. and Hero, A. O. (2017). Multilayer spectral graph clustering via convex layer aggregation: Theory and algorithms. *IEEE Transactions on Signal and Information Processing over Networks*, 3(3):553–567.

Culot, G., Nassimbeni, G., Orzes, G., and Sartor, M. (2020). Behind the definition of Industry 4.0: Analysis and open questions. *International Journal of Production Economics*, 226.

da Rosa Righi, R., Alberti, A. M., and Singh, M. (2020). *Blockchain Technology for Industry 4.0*. Springer.

Dasiopoulou, S., Saathoff, C., Mylonas, P., Avrithis, Y., Kompatsiaris, Y., Staab, S., and Strinztis, M. G. (2008). Introducing context and reasoning in visual content analysis: An ontology-based framework. In *Semantic Multimedia and Ontologies*, pages 99–122. Springer.

Drakopoulos, G., Kafeza, E., Mylonas, P., and Iliadis, L. (2021). Transform-based graph topology similarity metrics. *NCAA*, 1(1).

Drakopoulos, G. and Mylonas, P. (2020). Evaluating graph resilience with tensor stack networks: A keras implementation. *NCAA*, 32(9):4161–4176.

Egger, A., ter Hofstede, A. H., Kratsch, W., Leemans, S. J., Röglinger, M., and Wynn, M. T. (2020). Bot log mining: Using logs from robotic process automation for process mining. In *International Conference on Conceptual Modeling*, pages 51–61. Springer.

Halnaut, A., Giot, R., Bourqui, R., and Auber, D. (2020). Deep dive into deep neural networks with flows. In *VISIGRAPP*, volume 3, pages 231–239.

Kontopoulos, S. and Drakopoulos, G. (2014). A space efficient scheme for graph representation. In *ICTAI*, pages 299–303. IEEE.

Lopes, I. F. and Ferreira, D. R. (2019). A survey of process mining competitions: The BPI challenges 2011–2018. In *International Conference on Business Process Management*, pages 263–274. Springer.

Mandke, K., Meier, J., Brookes, M. J., O'Dea, R. D., Van Mieghem, P., Stam, C. J., Hillebrand, A., and Tewarie, P. (2018). Comparing multilayer brain networks between groups: Introducing graph metrics and recommendations. *NeuroImage*, 166:371–384.

McGee, F., Ghoniem, M., Melançon, G., Otjacques, B., and Pinaud, B. (2019). The state of the art in multilayer network visualization. In *Computer Graphics Forum*, pages 125–149. Wiley Online Library.

Mercado, P., Tudisco, F., and Hein, M. (2019). Generalized matrix means for semi-supervised learning with multilayer graphs. *arXiv preprint arXiv:1910.13951*.

Metcalfe, B. (2013). Metcalfe's law after 40 years of Ethernet. *Computer*, 46(12):26–31.

Mitsyuk, A. A., Shugurov, I. S., Kalenkova, A. A., and van der Aalst, W. M. (2017). Generating event logs for high-level process models. *Simulation Modelling Practice and Theory*, 74:1–16.

Rajput, S. and Singh, S. P. (2019). Connecting circular economy and Industry 4.0. *International Journal of Information Management*, 49:98–113.

Reinkemeyer, L. (2020). *Process Mining in Action: Principles, Use Cases and Outlook*. Springer Nature.

Souza, M. L. H., da Costa, C. A., de Oliveira Ramos, G., and da Rosa Righi, R. (2020). A survey on decision-making based on system reliability in the context of Industry 4.0. *Journal of Manufacturing Systems*, 56:133–156.

Suriadi, S., Andrews, R., ter Hofstede, A. H., and Wynn, M. T. (2017). Event log imperfection patterns for process mining: Towards a systematic approach to cleaning event logs. *Information Systems*, 64:132–150.

Tversky, A. (1977). Features of similarity. *Psychological Review*, 84(4):327.

Verenich, I., Dumas, M., Rosa, M. L., Maggi, F. M., and Teinemaa, I. (2019). Survey and cross-benchmark comparison of remaining time prediction methods in business process monitoring. *ACM TIST*, 10(4):1–34.

Wang, T., Ji, Z., Sun, Q., Chen, Q., and Jing, X.-Y. (2016). Interactive multilabel image segmentation via robust multilayer graph constraints. *IEEE Transactions on Multimedia*, 18(12):2358–2371.

Xie, C., Yu, B., Zeng, Z., Yang, Y., and Liu, Q. (2020). Multilayer Internet-of-Things middleware based on knowledge graph. *IEEE Internet of Things Journal*, 8(4):2635–2648.

Zerbino, P., Aloini, D., Dulmin, R., and Mininno, V. (2018). Process-mining-enabled audit of information systems: Methodology and an application. *Expert Systems with Applications*, 110:80–92.

Zhou, Y. and Cheung, Y.-m. (2019). Bayesian low-tubal-rank robust tensor factorization with multi-rank determination. *IEEE TPAMI*.